

# Numerical simulation of liquid-layer breakup on a moving wall due to an impinging jet

By T. Yu<sup>†</sup>, J. Park<sup>†</sup>, H. Moon<sup>†</sup>, J. Shim<sup>†</sup>, D. You<sup>†</sup>, D. Kim<sup>‡</sup>,  
AND A. Ovsyannikov

Jet-wiping is a hydrodynamic method for controlling the liquid film thickness in a coating process. In industrial conditions, the jet is generally turbulent. When the jet wipes a liquid film, it usually induces violent film instability called splashing. The instability is characterized by the ejection of droplets from the runback flow. Consequently, it can degrade the final coating quality since some of droplets can be reattached to the liquid film. The simulation result shows the main features of the liquid-layer breakup due to an impinging jet such as droplet trajectories.

---

## 1. Introduction

Jet-wiping is a hydrodynamic technique to manipulate the liquid thickness on a solid substrate, which is often utilized in a variety of industrial processes such as the galvanization process of a steel company. In a process for the galvanization of steel strips, known as a hot-dip coating process, a solid substrate is dipped into the bath of the coating fluid and is withdrawn so that both sides of the substrate are fully wetted with the coating fluid. While the wetted substrate is vertically moved, an air jet through a slot nozzle is applied to cut out excessive fluid and to achieve a required thickness of the coated liquid layer.

The pressure gradient and shear stress due to impingement of the turbulent slot jet on the liquid film not only reduce the thickness of the liquid film but also induce instability of the liquid film, resulting in splash of small droplets as illustrated in Figure 1. The splashing phenomenon on a liquid film often degrades the final quality of the coated surface since some of the droplets can be reattached to the film and produce pimples. Also some of droplets can be directed to the slot nozzle and collide with liquid film along the air jet path. This procedure can cause serious damage to the substrate surface and prevent from obtaining the desired liquid film thickness. In a severe situation, the interaction between the gas jet and the liquid film causes system-wise instability where the overall process becomes unstable and main wiping parameters are negatively affected.

Analytical and numerical methods have been employed to understand the main features of the interaction between an air jet and liquid film in coating processes (Myrillas *et al.* 2009, 2013). However, until recently, only a few attempts have been tried to characterize the liquid-layer breakup and instability. Volume-of-fluid (VOF) based simulations were performed to predict the splash phenomenon, however, the shape and distribution of the droplets appear qualitatively different (Lacanette *et al.* 2006). A theoretical model was suggested by Buchlin *et al.* (2003), however, neglects effects of the inertial force. Thus, the detailed flow physics during the liquid-layer breakup due to an impinging jet is neither

<sup>†</sup> Pohang University of Science and Technology (POSTECH), S. Korea

<sup>‡</sup> Cascade Technologies Inc.

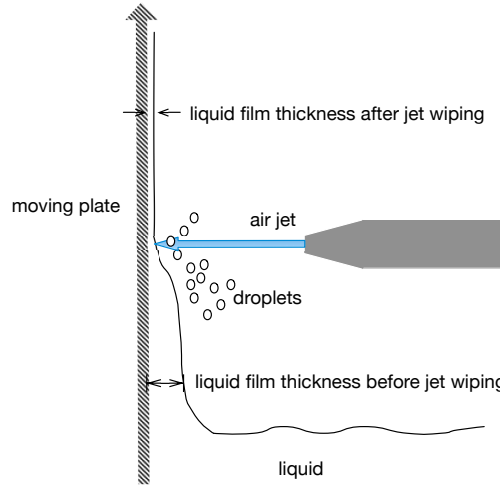


FIGURE 1. Schematic illustration of a jet-wiping process.

well predicted nor understood. Indeed, numerical simulations of the jet-wiping process pose a number of challenging technical issues associated with simulations of two-phase flows with high density, momentum, and viscosity ratios.

The present work aims at accurately predicting and gaining understanding of the liquid-film breakup and the spatial and temporal traces of the resulting minuscule liquid droplets. The technical challenges mentioned above are tackled with recent advancements in the VOF method. An unstructured-grid un-split geometric VOF scheme, developed at Cascade Technologies Inc., is employed (Kim *et al.* 2013). The VOF approach is coupled with the incompressible flow solver Cliff to predict unsteady interaction between the high-speed impinging air jet and a moving liquid film.

## 2. Flow configuration

The flow configuration is schematically illustrated in Figure 1 and consists of an upward moving substrate dragging a liquid layer through the viscous force from the bottom liquid bath and a nozzle ejecting the high-speed impinging jet toward the moving wall.

A computational grid initially consisting of 303,200 quadrilateral cells is constructed. In order to accurately capture the liquid-film breakup and the splashing phenomenon, the mesh resolution around the air jet, along the liquid film region, and jet impinging zone, are refined by a mesh adaptation technique called Adapt, as shown in Figure 2.

A no-slip boundary condition is imposed on the bottom wall, on the moving substrate wall, and on the jet nozzle wall. The convective outflow condition and/or the Neumann condition are applied at the exit/entrainment regions of the computational domain. Two-dimensional computations are carried out by imposing periodic boundary conditions in the spanwise direction.

The air jet is ejected from the nozzle exit with a polynomial velocity profile while the speed of the substrate wall is fixed to a constant. The ratio between jet nozzle speed and the substrate wall is 27. The Reynolds number of jet is 19,726 based on the nozzle slot width and the exit velocity. The Weber number is 13,538 based on the surface tension of the liquid. The density and viscosity ratio of liquid to air are 920 and 70, respectively,

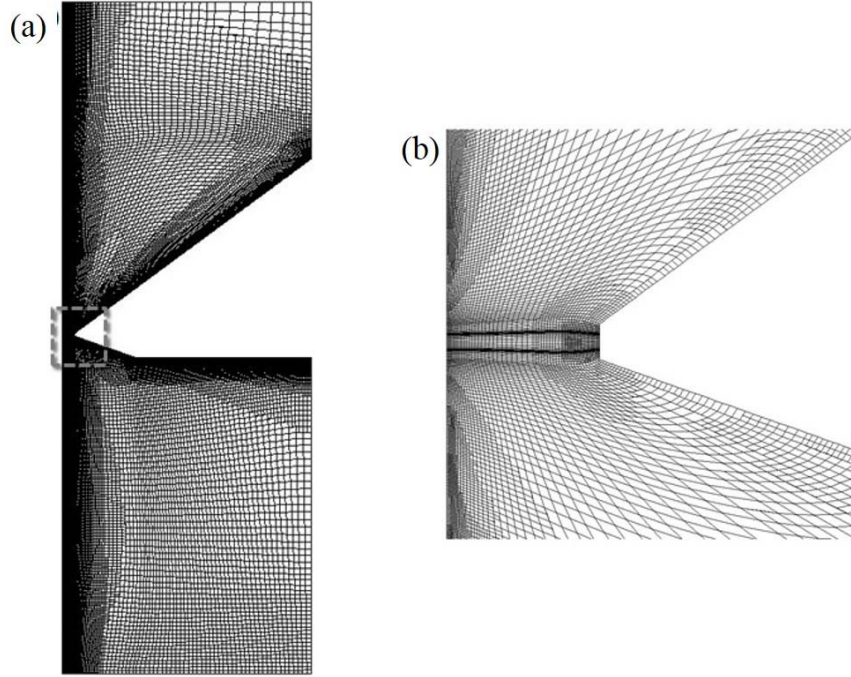


FIGURE 2. Computational grid used in the present simulations. (a) Whole computational domain and (b) near the jet exit.

at room temperature. The time-step size is adjusted during the simulation such that the CFL number is maintained at 1.0.

### 3. Numerical methods

The governing equations solved for the prediction of flows in the present configuration are the incompressible, immiscible Navier-Stokes equations for two-phase flows as follows

$$\frac{\partial \rho \mathbf{u}}{\partial t} + \nabla \cdot \rho \mathbf{u} \mathbf{u} = -\nabla p + \nabla \cdot \boldsymbol{\tau} + \mathbf{T}_\sigma + \rho \mathbf{g}, \quad (3.1)$$

$$\nabla \cdot \mathbf{u} = 0, \quad (3.2)$$

where  $\rho$  is the density,  $\mathbf{u}$  the fluid velocity,  $p$  the pressure,  $\boldsymbol{\tau}$  the viscous stress tensor,  $\mathbf{T}_\sigma$  is the surface tension force and  $\mathbf{g}$  is the acceleration of gravity. The density  $\rho$  and the viscosity  $\mu$  in a cell  $i$  are defined as volume averaged quantities

$$\rho_i = \mathbf{c}_i \rho_l + (1 - \mathbf{c}_i) \rho_g, \quad (3.3)$$

$$\mu_i = \mathbf{c}_i \mu_l + (1 - \mathbf{c}_i) \mu_g, \quad (3.4)$$

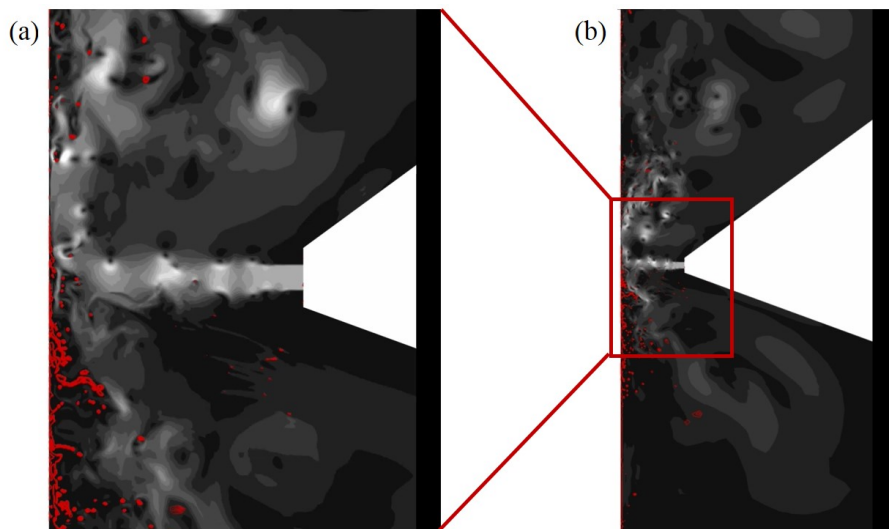


FIGURE 3. Interaction between a liquid-layer and an air jet producing droplet splash predicted by the present simulation (a) near the impinging jet region and (b) in the far field.

where  $c(\mathbf{x}, t)$  is the volume fraction which takes values between zero and one. Here, the subscript  $l$  denotes quantities in the liquid and the subscript  $g$  denotes those in the gas phase. The interface motion is described in terms of the volume fraction as follows

$$\frac{\partial c}{\partial t} + \nabla \cdot (\mathbf{c}\mathbf{u}) = 0. \quad (3.5)$$

In the present method, as mentioned earlier, Eq. (3.5) is solved using an un-split geometric advection scheme. Unlike the conventional flux-splitting VOF schemes, where successive one-dimensional advection steps are performed for calculating multidimensional advection and, therefore, suffer from numerical errors accumulated during the flux-splitting steps, the present un-split scheme computes the advection of a certain amount of fluid volume at a step by utilizing a geometrical way and allows exact conservation of the advected fluid mass.

#### 4. Results and discussion

The computation is initiated by simulating liquid flow on an upward moving plate without ejecting an air jet. Once the liquid film is fully developed on the moving wall, an air jet is ejected and impinges on the wall while it cuts out some of the liquid dragged along the moving wall. The simulation result shows the main features of the liquid-layer breakup due to jet-wiping as shown in Figure 3. Figure 4 shows the averaged thickness of liquid film. The liquid film thickness after jet-wiping is found to be about 10% of the thickness before jet-wiping.

While an air jet impinges the liquid film, not only does the thickness of the liquid film decrease but also a highly unstable region is created, as shown in Figure 3. A chaotic breakup process occurs due to an instability from interaction between turbulent jet flow and the thin liquid film. Also, numerous minuscule splash droplets from the runback flow cause another difficulty. This phenomenon often limits the applicability of the jet-wiping process since it can degrade the quality of the coated surface.

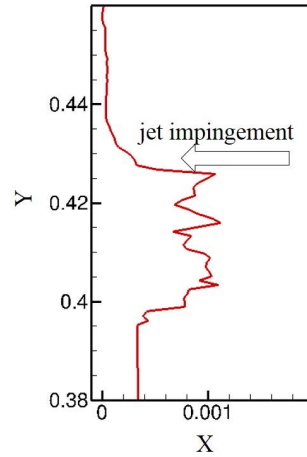


FIGURE 4. Averaged liquid film thicknesses near the jet impingement zone.

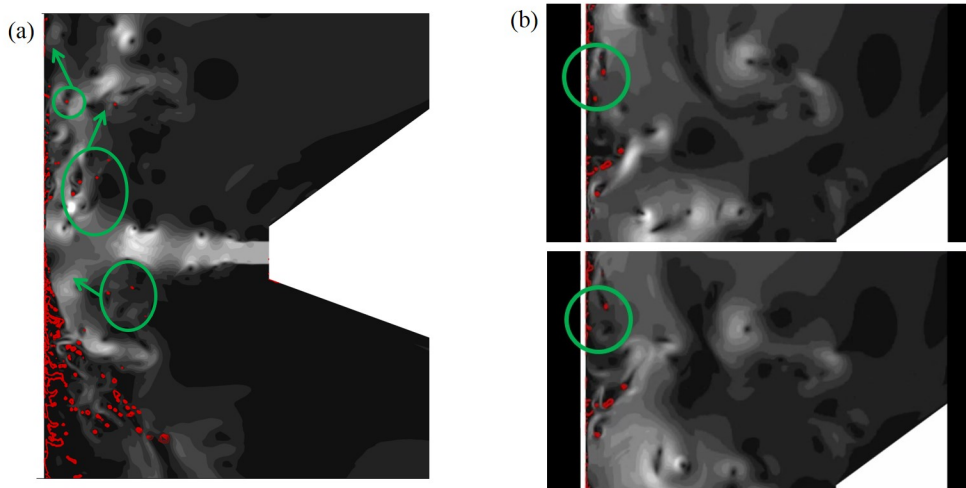


FIGURE 5. Characteristics of droplet trajectories. Figure shows (a) three types of droplet trajectories and (b) the resulting pimples.

The splashing mechanism of a liquid film is associated with the dynamic balance among the surface tension force, the viscous shear force, and the gravitational force. While runback flow from the impinging jet propagates along the solid strip, the force imbalance induces instability of the liquid film so that interface waves are corrugated resulting in breakup of the liquid film.

Due to the upward movement of substrate wall, splashing of liquid droplets in the present jet-wiping process is not symmetric above and below the impinging jet region. It is observed that breakup occurs more frequently below the impinging jet region because of both the gravitational force and the runback flow. The runback flow prevents the strip from conveying the liquid upward. As a result, the mass flow of liquid below the impinging

jet region is much larger than that above the impinging point. Thus, droplets are more abundant below the impinging jet region, and various size of droplets are observed.

Figure 5 illustrates the several features of the droplet trajectories. Gravity and buoyancy forces acting on droplets cause diverse motions. Larger droplets below the impinging jet point fall down toward the bath of coating liquid due to the gravitational force. On the other hand, small droplets show complicate behaviors.

Three types of droplet trajectories are observed from Figure 5(a). Small droplets below the impinging jet region follow the air stream in a circulating motion and collide with the liquid film along the air jet path. The droplets are directed to the liquid film by the air jet at high speed. Consequently, they deliver extra momentum along the air jet direction that causes damage on the liquid film surface. A number of droplets above the impinging jet follow the air stream and become reattached to the liquid film as shown in Figure 5(b), which leads to a local increase in the liquid-layer thickness.

## 5. Concluding remarks

In this study, an unstructured-grid un-split geometric VOF numerical technique is utilized that shows potential for investigating the liquid-layer breakup due to an impinging air turbulent jet. The simulations reveal intricate droplet trajectories as a result of the breakup of the liquid layer. In particular, small droplets above the impinging jet region reattach to the film, thereby leading to pimples, while the larger droplets fall due to the gravitational force. Additional simulations are currently being performed to exploit the full capabilities of the method.

### *Acknowledgments*

This work was supported by POSCO and the Brain Korea 21 Plus Project in 2014. The authors acknowledge valuable discussion with Dr. Dongeun Lee at POSCO. The authors acknowledge use of computational resources from the Certainty cluster awarded by the National Science Foundation to CTR.

### REFERENCES

- BUCHLIN, J.-M., GOSSET, A., V.PERROT, DUBOIS, M. & ANTHOINE, J. 2003 Effect of nozzle angle on splashing in jet wiping. In *Proceedings of 5<sup>th</sup> European Coating Symposium*.
- KIM, D., MANI, A. & MOIN, P. 2013 Numerical simulation of bubble formation by breaking waves in turbulent two-phase couette flow. *Annual Research Briefs*, Center for Turbulence Research, Stanford University, pp. 37–46.
- LACANETTE, D., GOSSET, A., VINCENT, S., BUCHLIN, J.-M. & ARQUIS, E. 2006 Macroscopic analysis of gas-jet wiping: Numerical simulation and experimental approach. *Phys. Fluids* **18**, 042103.
- MYRILLAS, K., GOSSET, A., RAMBAUD, P. & BUCHLIN, J. M. 2009 Cfd simulation of gas-jet wiping process. *Eur. Phys. J. Special Topics* **166**, 93–97.
- MYRILLAS, K., RAMBAUD, P., MATAGINE, J.-M., GARDIN, P., VINCENT, S. & BUCHLIN, J. M. 2013 Numerical modeling of gas-jet wiping process. *Chem. Eng. Proc.* **68**, 26–31.